

Histopathological analysis of residual lens cells in capsular opacities after cataract surgery using objective software

Christina Mastromonaco, Matthew Balazsi¹, Jacqueline Coblentz, Ana Beatriz Toledo Dias, Pablo Zoroquiain, Miguel N Burnier Jr

Purpose: Remnant lens epithelial cells (LECs) within the capsular bag (CB) undergo epithelial-to-mesenchymal transition (EMT) and acquire a myofibroblast phenotype, depositing extracellular matrix (ECM) components, leading to posterior capsular opacification (PCO). This study histopathologically analyzes the LEC-to-myofibroblast transition and *de novo* ECM component deposition (i.e., smooth muscle actin (SMA) and fibronectin (FN) expression) and determines the intraocular lens (IOL) and patient factors associated with these changes. **Methods:** In total, 190 CBs with IOLs were removed from donor eyes. Digital images were obtained, and PCO was graded using published software (ADOS, Medical Parachute). Automated immunohistochemistry was performed using anti-SMA to detect EMT and anti-FN to document ECM remodeling. Slides were digitized and analyzed using the Positive Pixel Count v9 algorithm. Linear regression and Poisson regression were performed ($P < 0.05$). **Results:** SMA positive expression decreased as the time of IOL implantation increased ($P < 0.0001$). Positivity of SMA and FN demonstrated a positive correlation ($P = 0.0002$). Controlling for confounding factors in Poisson regression, hydrophobic and hydrophilic materials showed higher FN and SMA expression when compared to silicone material lenses (FN; $P = 0.018$; $P < 0.0001$, SMA; $P = 0.001$; $P = 0.003$, respectively). The square optic design had 29% higher SMA positivity compared to the opti-edge design ($P = 0.042$). One-piece haptic lenses had higher SMA expression compared to three-piece haptic ($P = 0.042$). A higher risk of expression of SMA and FN was seen in patients with a history of smoking, hypertension, and glaucoma ($P < 0.05$). **Conclusion:** This study demonstrated that SMA and FN expression is different according to IOL design and patient factors, thus indicating that LEC changes depend on lens biocompatibility. Therefore, by analyzing the histopathological composition of PCO by using LECs, further insight into the characteristics of IOLs that are important for biocompatibility can be ascertained.

Key words: Capsular opacification, immunohistochemistry, intraocular lens, objective software, post-mortem eyes

Cataracts are the leading cause of blindness worldwide, significantly impairing a person's ability to perform daily tasks, thereby negatively impacting the quality of life.^[1] Vision, however, can be restored through cataract surgery, which involves the replacement of the crystalline lens with an intraocular lens (IOL) implant within the capsular bag (CB). It is estimated that the number of cataract surgeries performed in 1 year ranges 4000–10,000 per million in developed countries and 500–2000 per million in developing countries.^[2]

Surgical cataract extraction and implantation of an IOL, however, provokes an injury-like response within the eye from the disruption of the blood–aqueous barrier, leading to foreign body reactions.^[3] The rupture of the anterior capsule basement membrane through the capsulorhexis leads to a loss

of cell-to-cell contact between the lens epithelial cells (LECs), resulting in wound healing repair mechanistic activation. Macrophage and giant cell infiltrates secrete many cytokines to stimulate and promote the remnant LECs within the capsular bag to undergo epithelial-to-mesenchymal transition (EMT) like-changes toward a myofibroblastic phenotype.^[3,4] The myofibroblasts produce contractile forces and are characterized by their expression of α -smooth muscle actin (α -SMA), which are significantly increased after capsular rupture and typically not expressed in normal lenses.^[5-8] Moreover, myofibroblasts initiate a fibrotic reaction secreting fibrous extracellular matrix (ECM), which include collagen, proteoglycan, laminin, and fibronectin (FN).^[3,8,9] Furthermore, lens fibers can rearrange themselves into Soemmering's ring (SR) formations in the periphery of the CB. Altogether, these reactions lead to

This is an open access journal, and articles are distributed under the terms of the Creative Commons Attribution-NonCommercial-ShareAlike 4.0 License, which allows others to remix, tweak, and build upon the work non-commercially, as long as appropriate credit is given and the new creations are licensed under the identical terms.

For reprints contact: WKHLRPMedknow_reprints@wolterskluwer.com

Cite this article as: Mastromonaco C, Balazsi M, Coblentz J, Dias AB, Zoroquiain P, Burnier Jr MN. Histopathological analysis of residual lens cells in capsular opacities after cataract surgery using objective software. Indian J Ophthalmol 2022;70:1617-25.

Department of Pathology and Ophthalmology, The MUHC-McGill University Ocular Pathology Laboratory, Montreal, Quebec, ¹Medical Parachute, Montreal, Quebec, Canada

Correspondence to: Dr. Christina Mastromonaco, Department of Pathology and Ophthalmology, The MUHC-McGill University Ocular Pathology Laboratory, Montreal, Quebec, Canada. E-mail: Christina.mastromonaco@mail.mcgill.ca

Received: 03-Feb-2021

Revision: 07-Jun-2021

Accepted: 23-Jan-2022

Published: 28-Apr-2022

Access this article online

Website:

www.ijo.in

DOI:

10.4103/ijo.IJO_291_21

Quick Response Code:



the formation of capsular opacifications, further leading to impairment of vision.

Studies suggest that biocompatibility of the IOL implant is a factor that contributes to the extent of the wound healing reaction seen within the CB and can impact the formation of the capsular opacities.^[10-13] Linnola *et al.* suggest a potential correlation between FN adhesion to the IOL and posterior capsular opacification (PCO) formation amongst IOL materials, further supporting that FN is a mediator between LECs and the IOL surface.^[12,14] Matsushima *et al.*^[11] demonstrated the importance of material and optic edge design on PCO by using animal model studies and suggest the use of cytoskeletal proteins as a potential therapeutic target for PCO. Moreover, Saika *et al.*^[13] noticed the expression of α SMA in different IOL materials but with no correlation studies documentation in regards to the time of IOL implantation and its effect on the histological differences between IOL materials.

Biocompatibility between the IOL implant is an important concept to define as many factors are involved. Biocompatibility, in this case, can be defined as the biological reaction of the LECs and capsular bag components toward the non-biological materials of the IOL. All factors that can influence this biocompatibility of the IOL are factors that include but are not limited to the patient and the IOL characteristics. The aim of this study is to define if there are IOL factors (optic edge design, material, haptics, and filter) and patient factors (age, smoking history, diabetes, hypertension, glaucoma, and history of cancer) that are associated with the expression of myofibroblastic changes seen in EMT (SMA and FN expression) and capsular opacities through histopathological analyses. We further aim to standardize our grading through software analysis for both immunohistochemical analysis and opacification scores.

Methods

In total, 190 post-mortem donor eyes implanted with IOLs fixed in 10% formalin were obtained from the Minnesota Lions Eye Bank (Saint Paul, MN, US). All data accumulation was in accordance with the Canada and Province of Quebec legislation and the tenets of the Declaration of Helsinki. All eyes were sectioned across the coronal axis, posterior to the CB, for gross pathological examination. Under the Leica EZ4HD (Wetzlar, Hesse, Germany) stereomicroscope, zonulas of the eye were cut carefully using Westcott scissors to remove the CB with the implanted IOL.

The CBs were imaged using the Olympus DSX110 digital microscope (Philadelphia, PA, USA). Lighting conditions were set at full trans-illumination brightness, and a standardized lighting condition was used for CB images. Opacities of the CB were graded on the images by using a previously published automated detector opacification software (ADOS) by Medical Parachute (Montreal, QC, Canada).^[15] ADOS software quantification scored CB opacities through a luminosity score, which represented the intensity of the opacification, and CB opacity area (in percentage).

CB tissue was sectioned in half through the haptic locations. Specimens were processed routinely and paraffin-embedded to visualize the anterior and posterior capsular tissue on the histology slide. Fully automated immunohistochemistry

using the Ventana Benchmark Automated Platform was performed according to the manufacturer's recommended protocol (Ventana Medical Systems, Tucson, AZ). Processing of the barcoded slides included baking, solvent-free deparaffinization, and CCI (Tris-EDTA buffer pH 8.0)-based antigen retrieval. The slides were then incubated with anti-SMA (Dako clone 1A4) and anti-FN (Abcam ab32419) at a dilution of 1:300 for 30 min at 37°C, followed by the addition of biotinylated secondary specific antibodies, and of an avidin/streptavidin-coupled alkaline phosphatase enzyme conjugate. Signals were visualized with Fast Red (Ventana, Tucson, AZ) as a chromogenic substrate, and slides were then counterstained with hematoxylin. Normal colon sections were used as positive controls for SMA and normal intestine as a positive control for fibronectin; the primary antibody was omitted for negative controls.

Slides were digitized using the Aperio ScanScope Scanner (Aperio AT Turbo, Leica Biosystems Imaging, Inc). By using the digital slides, a section of the capsular bag tissue was demarcated; this area included the anterior and posterior capsule, the SR, and the IOL space [Fig. 1]. IOL biomaterial was noted to melt away during the embedding process of the tissue, leaving a defined empty area, which corresponded to the IOL placement. By using the Positive Pixel Count v9 algorithm (Aperio ImageScope) software set at a hue value of 0.878, the positivity (total number of positive/total number of pixels \times 100, mm²) was obtained [Fig. 2].

To assess the time of IOL implant with the expression of SMA and FN and with the opacity outcomes (overall intensity and area), a regression analysis was used to identify any associations. Univariate and multivariate Poisson regression analyses were performed to assess the relationship between IOL factors (optic edge design, material, haptics, and filter), patient factors (age, smoking history, diabetes, hypertension, glaucoma, and history of cancer), and expression of FN and SMA. Incidence rate ratios (IRRs) were calculated, and $P < 0.05$ was considered statistically significant. Statistical analyses were performed using STATA14.2 (Stat Corp. TX).

Results

Initially, 190 post-mortem donor eyes were pathologically grossed. Once slides were digitalized, 86 samples were excluded from our data set due to the inability to clearly visualize both anterior and posterior capsular tissue after embedding. CB histology sections allowed for visualization of the SR composition within the CB basement membrane, which surrounds the edge of the IOL optic. CB images demonstrated a clear view of the opacities within the capsular bag [Fig. 1].

We were unable to obtain the IOL model number of one sample; thus, 103 eye specimens were retained for the final analyses. The average time between patient's cataract surgery and death of the patient (post-IOL implantation) was 62.5 ± 47.6 months, which ranged between 3 and 226 months. The average age of the patient at the time of cataract surgery was 76.6 ± 8.2 years. The mean age of patients when deceased was 81.8 ± 7.8 years. The male: female ratio was 59:44. There were 4.8% (5) patients classified as smokers, 10.6% (11) as diabetics, 19.4% (20) with hypertension, and 20.3% (21) were diagnosed with cancer at some point in their lifetime.

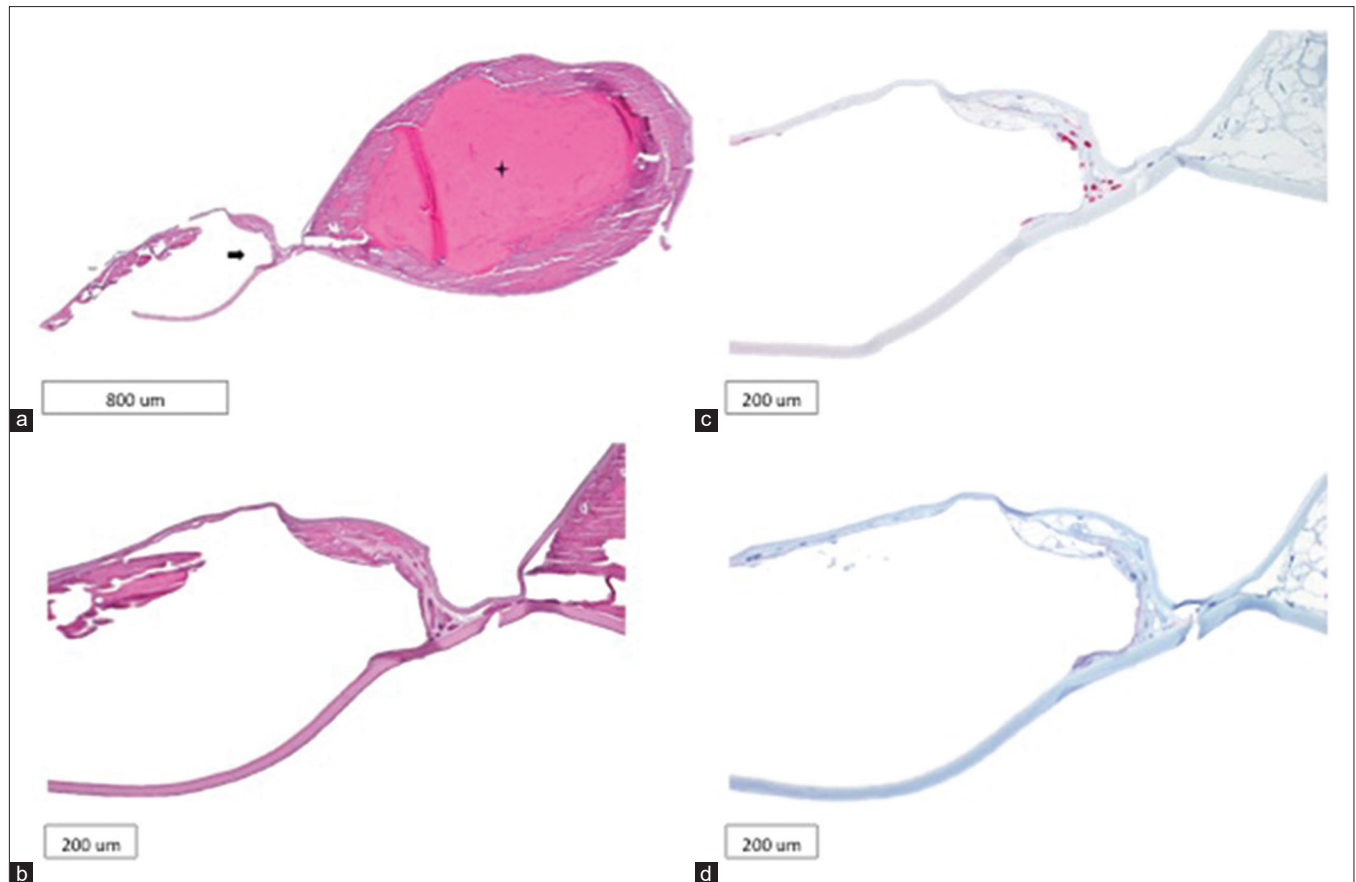


Figure 1: Histological sections of capsular bag tissue. a) Hematoxylin and eosin stain demonstrated the anterior (bottom basement member) and posterior capsule (top basement membrane). Soemmering’s Ring opacities are located in the bulk, indicated with the star. Placement of the optic edge of the intraocular lens is indicated with the arrow. b) Magnification of the intraocular lens placement between the anterior and posterior capsule. c) Immunohistochemistry of α -smooth alpha-actin on the capsular bag tissue. d) Immunohistochemistry of fibronectin on the capsular bag tissue

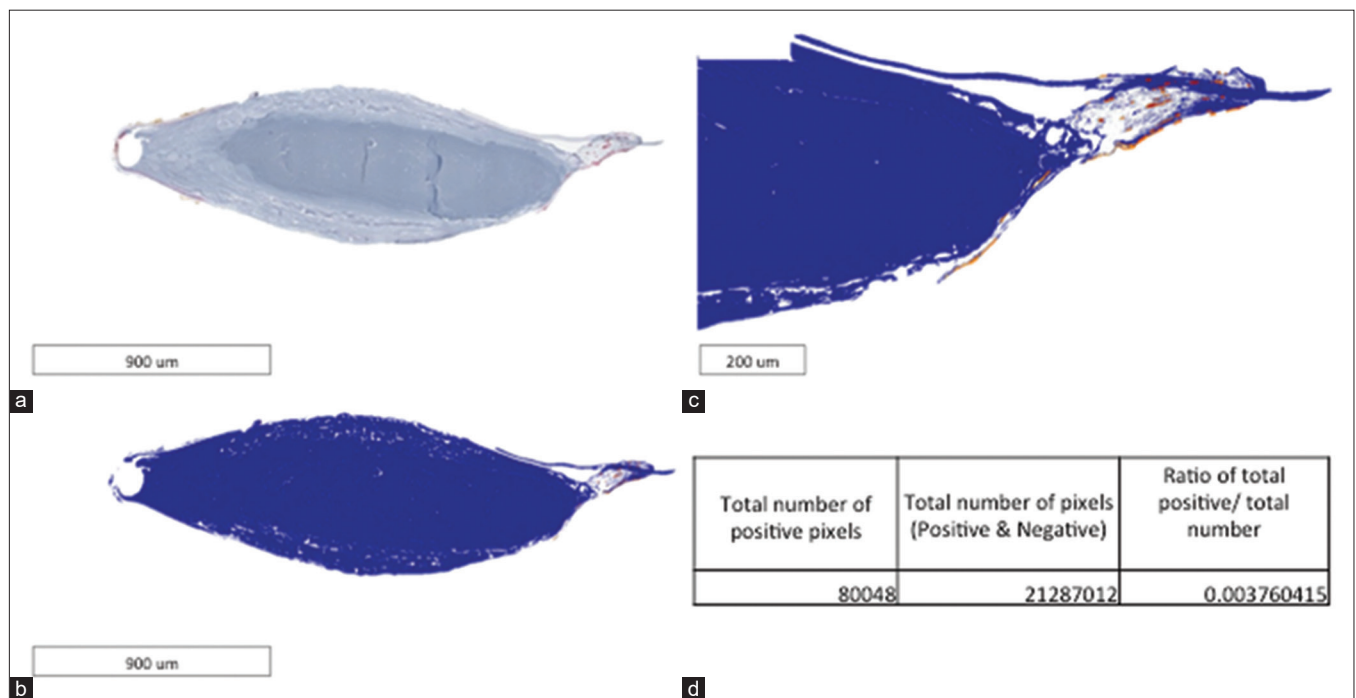


Figure 2: Digital slide of the capsular bag with quantification algorithm. a) Capsular bag stain smooth alpha-actin (SMA). b) Positive Pixel Count v9 algorithm quantification on the Aperio ImageScope. Blue indicates negative staining, orange indicates positivity, and red indicates strong positive staining. c) Magnification of the edge of the intraocular lens placement. d) Positive Pixel Count data output for SMA expression

Table 1: Impact of IOL time (months) on the outcomes (FN and SMA expression and opacity)

	Univariate			Multivariate		
	Beta	95% CI	P	Beta	95% CI	P
FN positivity	-1.05	-2.19-0.086	0.069	-0.43	-1.70-0.84	0.499
SMA positivity	-4.56	-6.12--3.12	0.0001	-2.67	-4.02--1.33	0.000
Overall Opacityarea	0.037	-0.089	0.098	0.04	-0.021-0.1	0.182
Overall Opacityintensity	2.04	1.04-3.03	0.0001	1.89	0.55-3.23	0.009

Impact of IOL time (months) on the outcomes (FN and SMA expression, and opacity). IOL time has a significant association with the SMA positivity and Overall Opacityintensity after controlling for laterality, gender, age, smoking status, and medical history (diabetic, hypertension, AMD, glaucoma, and cancer). $P < 0.05$ was considered significant

Table 2: Impact of selected demographic and clinical characteristics on FN and SMA expression

	Smoking	Diabetics	Hypertension	Glaucoma	Cancer
FN positivity	4.68 (3.41-6.43)*	1.25 (0.92-1.71)	1.73 (1.34-2.22)*	3.16 (2.37-4.21)*	0.40 (0.27-0.60)*
SMA positivity	6.85 (5.45-8.61)*	0.58 (0.36-0.93)*	3.01 (2.47-3.65)*	7.56 (6.04-9.45)*	0.88 (0.69-1.13)

Impact of patient factors on the outcomes (FN and SMA expression). Estimates are adjusted for age and gender. Incident rate ratio (confidence interval), P values are significant at 5%

Table 3: Impact of various parameters on the SMA positivity by using Poisson Regression

Parameter	Univariate			Multivariate		
	IRR	95% CI	P	IRR	95% CI	P
Edge Design						
Optic	1.00			1.00		
Square	1.69	1.39-2.07	<0.0001	1.29	1.01-1.66	0.042
Material						
Silicone	1.00			1.00		
Hydrophobic	5.01	2.98-8.39	<0.0001	2.34	1.34-4.06	0.003
Hydrophilic	5.76	3.34-9.92	<0.0001	2.61	1.46-4.65	0.001
Haptics						
3 Piece	1.00			1.00		
1 Piece/Plate	1.69	1.39-2.07	<0.0001	1.30	1.01-1.67	0.042
Filter						
Clear	1.00			1.00		
Blue	0.44	0.32-0.60	<0.0001	0.8	0.56-1.13	0.208
Any Parameter						
None	1.00			1.00		
1-2	6.61	3.95-11.05	<0.0001	3.85	2.26-6.55	<0.0001
3-4	2.4	1.33-4.32	0.004	2.66	1.44-4.92	0.002

Impact of various parameters on the SMA positivity by using Poisson Regression. Multivariate analysis controlling for laterality, gender, age, smoking status, and medical history (diabetic, hypertension, AMD, glaucoma, and cancer). IRR=Incident rate ratio. $P < 0.05$ was considered significant

Two patients were diagnosed with age-related macular degeneration (AMD) (1.9%) and eight with glaucoma (7.7%).

Our cohort was composed of twelve different lens types: SN60WF (21), ZCB00 (19), ZA9003 (17), AR40/e (16), Z9002 (12), SA60AT (11), SI40NB (2), MI60L (1), FC-60AD (1), LI41U (1), SN6AT4 (1), and ZCT300 (1). From these samples, 55 had a square edge design (53%), 47 had an opti-edge design (rounded edge in the anterior and square edge in the posterior) (46%), and one had a round edge (1%). Seventy-one lenses were made from hydrophobic acrylic material (69%), 17 were hydrophilic acrylic (17%), and 15 were made from silicone (15%). Fifty-four lenses were one-piece design (53%), 48 were three-piece

design (47%) and one was a plate design (0.1%). Eighty-one samples were clear-filter lenses (73%), whereas 22 were blue-filter lenses (27%).

When we compared the opacity intensity and opacity area, we found that both variables displayed a positive correlation ($r = 0.503$, $P = 0.006$). Expression levels of SMA and FN demonstrated a positive correlation, indicating that epithelial-to-myofibroblastic transition (SMA expression) was accompanied by ECM remodeling (FN expression) ($r = 0.527$, $P = 0.0002$). In contrast, a negative correlation was observed between SMA expression and capsular opacities (both in area and intensity), suggesting a long-term loss of myofibroblasts

Table 4: Impact of various parameters on the FN positivity by using Poisson Regression

Parameter	Univariate			Multivariate		
	IRR	95% CI	P	IRR	95% CI	P
Edge Design						
Optic	1.00			1.00		
Square	1.67	1.32-2.12	<0.0001	1.28	0.99-1.66	0.064
Material						
Silicone	1.00			1.00		
Hydrophobic	3.21	1.95-5.27	<0.0001	1.92	1.12-3.28	0.018
Hydrophilic	3.52	2.06-6.03	<0.0001	2.87	1.61-5.10	<0.0001
Haptics						
3 Piece	1.00			1.00		
1 Piece/Plate	1.67	1.32-2.12	<0.0001	1.28	0.99-1.66	0.064
Filter						
Clear	1.00			1.00		
Blue	1.01	0.77-1.34	0.9143	1.19	0.87-1.65	0.273
Any Parameter						
None	1.00			1.00		
1-2	3.37	2.09-5.43	<0.0001	2.68	1.62-4.44	<0.0001
3-4	2.93	1.74-4.94	<0.0001	2.83	1.62-4.95	<0.0001

Impact of various parameters on the FN positivity using Poisson Regression. Multivariate analysis controlling for laterality, gender, age, smoking status, and medical history (diabetic, hypertension, AMD, glaucoma, and cancer). IRR=Incident rate ratio. $P < 0.05$ was considered significant

as opacities increase within the CB ($r = -0.564$, $P = 0.005$; $r = -0.435$, $P = 0.038$).

In addition, we sought to correlate the expression levels of SMA and FN in association with the time at which the IOL was implanted. We found that the expression of SMA decreased with time after IOL implantation within the CB, confirming a negative association by univariate regression analysis ($P = 0.0001$). A similar negative association was found in the multivariate regression analysis after controlling for laterality, gender, age, smoking status, and medical history ($P < 0.001$) [Table 1]. Notably, we observed that a longer IOL implant time was associated with an increase in overall opacity intensity by both the univariate ($P = 0.0001$) and multivariate analyses ($P = 0.009$) [Table 1]. No other significant associations were found between IOL implant time and other outcomes [Table 1].

Age as a factor on its own showed a negative association with SMA expression in the multivariate regression analysis (Beta = -0.28 , 95% CI = -0.29 to -0.069 , $P = 0.010$), and no association with FN expression.

In a sub-group analysis, the association between FN and SMA expression to patients' characteristics (smoking, diabetes, hypertension, glaucoma, and cancer) were analyzed following adjustments for age and sex. An increased risk of FN expression was observed in patients with passed smoking status (IRR = 4.68). Similar associations were observed in hypertensive and glaucoma patients (IRR = 1.73 and 3.16, respectively). However, FN expression risk was marginally decreased with the history of cancer (IRR = 0.40), while no association with regard to the history of diabetes was noted [Table 2]. In addition, patients who were smokers, hypertensive, or who had a history of glaucoma demonstrated slightly higher associations with SMA expression (IRR = 6.85,

3.01, and 7.56, respectively). A slight risk decrease in SMA expression was demonstrated in patients with a history of diabetes (IRR = 0.58), and no association was noted with the patient's history of cancer [Table 2].

On the contrary, four main characteristics of IOLs—lens optic edge design (optic and square), material (silicone, hydrophobic, and hydrophilic), haptic piece (3 piece and 1 piece), and lens filter (clear filter and blue filter)—were categorized and analyzed regarding the expression of SMA and FN. To this end, we used a Poisson regression analysis (univariate and multivariate) on each outcome. Using these analyses, we found that the square optic design IOL implant had a 69% higher risk of SMA positivity compared to the opti-edge design using univariate regression analysis and a 29% higher positivity after controlling for confounding factors in the multivariate analysis ($P < 0.0001$ and $P = 0.042$, respectively) [Table 3]. Also, hydrophobic and hydrophilic materials showed a 5.01 and 5.76 higher risk of SMA positivity when compared to silicone ($P < 0.0001$, univariate analysis). Higher risk of SMA positivity was still observed after adjusting for confounding factors ($P = 0.003$ and $P = 0.001$, respectively) [Table 3]. When we took the haptic into account, we found that the one-piece haptic lenses had higher SMA expression as compared to three-piece haptic by using either univariate and multivariate regression analysis ($P < 0.0001$ and $P = 0.042$, respectively) [Table 3]. Lenses with blue filters lenses showed a 0.44 times lower SMA expression when compared to clear-filter lenses ($P < 0.0001$) by using the univariate analysis; however, this difference did not reach significance when confounding factors were taken into account ($P = 0.208$) [Table 3]. Taking into consideration the combination of more than one IOL parameter, we observed consistent and significantly higher SMA expression [Table 3].

When taking into account FN expression, we found that square-edge IOL design was associated with a 67% higher risk of FN positivity compared to those implanted with the opti-edge design ($P < 0.0001$, univariate analysis). Significance was lost, however, after controlling for confounding parameters by using multivariate regression analysis [Table 4]. Also, both hydrophobic and hydrophilic materials demonstrated a 3.21 and 3.52 times higher risk in FN expression when compared to silicone ($P < 0.0001$, univariate analysis). This association was still present after controlling for confounding factors as demonstrated by a 1.92 and 2.87 times higher FN expression in comparison to silicone material lenses (hydrophobic: $P = 0.018$; hydrophilic: $P < 0.0001$) [Table 4]. One-piece haptic seemed to be associated with higher FN expression using univariate analysis; however, this difference was no longer significant after controlling for external factors in the multivariate analysis ($P < 0.0001$ and $P = 0.064$, respectively) [Table 4]. In contrast to SMA expression, the lens filter did not demonstrate any differences in FN expression [Table 4]. Taking into consideration the combination of more than one IOL parameter, we again observed consistent and significant higher FN expression ($P < 0.0001$ with both univariate and multivariate analyses) [Table 4].

The intensity of the opacities within the CB was also analyzed in regard to the IOL factors. We found that the intensity of the opacities was statistically high in the IOLs made with silicone material compared to those made with hydrophobic and hydrophilic materials, with hydrophilic material having the least amount of opacity intensity. (IRR = 0.51, $P < 0.001$, 95% CI = 0.38–0.74 and IRR = 0.40, $P = 0.001$, 95% CI = 0.23–0.69, respectively). After controlling for confounding factors, differences were no more significant. Moreover, we did not observe any correlation between the intensity of opacities and the other IOL parameters (i.e., edge design, haptic, and color filters).

Altogether, these analyses brought evidence that the IOL parameter affects to different extents the phenotypic behaviors and the opacities within the CB.

Discussion

Our study analyzed the associations between IOL factors and EMT changes post-cataract surgery by using immunohistochemical and objective software methods. To the best of our knowledge, this is the first time that IOL implantation time was analyzed in post-mortem human eyes and compared with EMT changes of the CB by using digital pathology software quantification.

Previous studies on capsular bag quantifications of ECM on histopathology slides have used different methodologies (such as SDS-PAGE and Western blot) and scoring techniques (such as gamma counter and light microscopy counting), and none have used software algorithms directly on the immuno digital slides.^[11–13,16] Accurate objective quantification of immunostaining is important for all cases in pathology. As CB tissue is relatively small, even the smallest staining differences between samples are important. Furthermore, due to the size and the elasticity of the tissue, it was quite difficult to embed the CB in a proper orientation and to obtain proper sections that allowed visualization of all structures. For this reason, our lab quantified the immune slides of the CB by using the Positive Pixel Count v9 algorithm provided by the

digital slide scanner. Our technique allows objective software protein quantification directly on the histology slides, identifying the protein expression without tissue disruption, and allowing for protein localization throughout the entire CB tissue section. The Positive Pixel Count v9 algorithm is a tool that can be adjusted with specific specifications by the user with any stained slide, regardless of color or expression levels, and has controlled variables across all samples. This algorithm allowed for non-bias quantification of both area and intensity of all slides in the exact same way in just a few minutes with a click on a button, in comparison to a traditional light microscopic analysis. The Positive Pixel Count algorithm can be a useful and quick tool to quantify the immunohistochemical expression in small tissue samples like the CB in both research and clinical settings. Pathology sectors have increasingly been using digital pathology tools for both patient diagnosis^[17,18] and research purposes in all research fields.^[19–21] Benefits of digital pathology scanned slides include but are not limited to higher picture quality, ability to view entire tissue sections at different magnifications, and facility to share images with users at another location through a web-based platform.^[17]

In the cohort we included in the present study, the period of time that the IOL had been implanted in the CB was obtained from medical records and allowed for an enhanced understanding of FN and SMA expression through time. Histopathological differences in the cellular and extracellular matrix (ECM) components in specimens may be affected by IOL time, as noted by Werner *et al.* in their study; however, no concrete conclusion could be made without the exact time of implant.^[22] Although EMT and ECM changes between lens materials have been demonstrated, Saika *et al.*^[13] point out that post-surgical IOL implantation time may be a defining factor for these tissue and cellular variables, which were not analyzed in their study. Furthermore, Ishibashi *et al.*^[23] concluded that post-surgical IOL implantation time is an important factor that affected the capsular opacity composition as they analyzed anterior subcapsular opacities in monkeys. They demonstrated that during the first 2 months post-operation, opacities were composed mostly of proliferating LECs, and at 12 months, most of the LECs degenerated with much higher levels of ECM. Our present observations are in line with their findings as we report herein a negative correlation between SMA expression and IOL implantation time, suggesting that EMT changes are highest within the first few months post-surgery and decrease with time, most likely due to cell loss or phenotypic reversion into an epithelial fate. Our results also suggest that there are viable cells even 15 years post-cataract surgery, which is consistent with the conclusions stated in Marcantonio *et al.*'s^[24] study, and further state that these cells are location independent within the capsule. The results from our samples were also validated when confounding factors such as age and medical history were added to the analysis, associating SMA expression to have a 2.67 times lower risk for every month post IOL implantation.

Patient factors in our cohort that were linked with a higher risk of expression of SMA and FN were seen in patients with a history of smoking, hypertension, and glaucoma. It is possible that these patient factors cause further changes in the ocular circulation and activate certain inflammatory markers, causing CB changes and increased protein expressions.^[25] It has been shown that ocular comorbidities, such as glaucoma, do

contribute to a higher risk of PCO development.^[26] Chen *et al.*^[26] suggested that elevated intraocular pressure (IOP) in glaucoma patients may result in changes in LEC biology and CB structure. Moreover, Hoehn *et al.*^[27] demonstrated in the Gutenberg Health Study that their multivariate analysis revealed a correlation between hypertension, smoking, and higher IOP. This suggests an association between patient factors that result in elevated IOP and possible changes in LECs. Our study demonstrates that intra-capsule composition can be changed based on patient factors, all of which are important to note prior to IOL selection to reduce PCO development. Future studies with a larger cohort of patients are being assessed currently by our group for statistical comparison between patient factors and PCO development.

It is well demonstrated that PCO severity can significantly vary by different IOL materials.^[10] In addition, a study conducted by Saika *et al.*^[13] illustrated that SMA expression was observed throughout all types of IOL materials. In our study, we deepened these analyses by considering different IOL parameters. We observed in our cohort that the opti-edge design with silicone three-piece haptic models had the lowest SMA expression. The factor of time may allow for an understanding as to why SMA was lower in the opti-edge design with silicone three-piece haptic models. A negative correlation was demonstrated between SMA expression and IOL implant time, and SMA was at higher levels in the first few months of implantation. In general, most of the longer IOL implants were typically of the silicone three-piece haptic models; therefore, newer models such as the square, blue-light filtering one-piece designs had an average of a shorter implant time. As SMA expression is higher in the first few months of surgery, those lenses are signifying a higher SMA at that specific time point of when the tissue was fixated.

Not many studies have compared different expression levels of SMA between IOL models, and a most recent study did not show SMA differences between two similar lens types;^[28] therefore, further studies in the literature are required. Although we did not statistically analyze the location of SMA expression, we did find overall that SMA expression was present mostly between the optic-haptic junction. Marcantonio *et al.*^[24] confirmed in their study that SMA positivity was found around the capsulorhexis and that this alignment may lead to contractions of these cells, causing retraction off the IOL and potentially leading to IOL decentration. Further studies are warranted to analyze the relationship between SMA positivity and decentration of different IOLs.

Our results further demonstrated a negative correlation between the opacities quantified through gross pathology by using the ADOS software and SMA expression. We suggest that most of the SMA expressing cells undergo EMT transitions prior to any opacity visualization. It is possible that after IOL surgery, LECs undergo EMT, migrate, and start expressing SMA during the first months and then either lose this marker and hence operate a mesenchymal-to-epithelial transition or simply die and lose this expression. As EMT cells seem to occur early on, opacities only become observable once most of these transformations have already occurred. We also observed that as the intensity of the opacities increased, so did the area of opacities observed within the capsular bag. The intensity of the opacities seemed to be significantly higher in silicone materials;

however, after controlling for confounding factors, it was no longer observed. We believe that a much larger sample size is needed to verify the significance of IOL factors that contribute to opacity formations.

FN is an important indicator and player during the inflammatory process, and its expression is known to increase during PCO development. Linnola *et al.* studied the role of FN as a mediator that allows for adhesion of the IOL with the CB, contributing to the presence of PCO on the different IOL materials.^[12,14] They concluded that FN is the primary ECM protein between the IOL surface and the CB, referring to this adhesion as the "sandwich" theory. Their results demonstrated that FN expression between the haptic-optic junction in the hydrophobic acrylic IOL materials is significantly higher compared to that in the case of PMMA and silicone IOLs. In addition, they observed that the acrylic lens had more LECs, signifying that acrylic IOLs had better adhesions in the CB. Cooke *et al.* demonstrated that LECs attach better to acrylic material IOLs and that a FN coating increases this effect in *in vitro* models.^[29] Our study did have similar findings, in that there was higher FN in the acrylic lens materials, with the highest FN expression in hydrophilic materials, thus agreeing that the composition of the acrylic lenses does embrace this attachment.

In the present study, we found that SMA expression positively correlates with FN expression, indicating that epithelial to myofibroblastic transition (SMA expression) was accompanied by ECM remodeling (FN expression). Studies have shown that SMA and FN expression have similar downstream effectors via induction by TGF- β ,^[30] such as connective tissue growth factor (CTGF), which contributes to the EMT and ECM pathogenesis and their synthesis.^[31,32] CTGFs may activate different pathways, as described by Ma *et al.*^[33] They demonstrated that CTGFs activate the ERK pathways and SMAD signaling to induce EMT-associated protein expression (i.e., SMA) and to promote fibrosis (FN production), respectively. Moreover, Mamuya *et al.* demonstrated that SMAD-3 expression can be stopped through the TGF- β cascade in a mice model that lacked α -integrin.^[34] They illustrated that the lack of α -integrin expression decreased FN in terms of promoting fibrotic PCO but did not find similar patterns with α -SMA expression. The authors proposed that an α -integrin therapeutic antagonist would prevent fibrotic PCO. However, other factors must be taken into consideration when targeting the expression of FN, one being the benefits of FN for capsular adhesion to the IOL.

Reactive oxygen species (ROS) are other factors that have been shown to cause a PCO phenotype in promoting LEC growth.^[35] Zukin *et al.*^[36] tested aldose reductase (AR) inhibition as a therapeutic target to decrease ROS production, leading to the prevention of PCO development. Mechanistically, they concluded that AR inhibition interferes in the TGF- β /SMAD pathway and inhibits the EMT, including the expression of SMA and FN. Therefore, different downstream effectors to TGF- β and SMAD or non-SMAD pathways seem to be more complex, and further studies need to be conducted to find a therapeutic that can target both EMT and fibrotic processes.

The limitations to this study include the CB tissue itself. Due to the small size and the elasticity of the CB, it was quite difficult to embed the CB in a proper orientation. This limited

our sample size as visualization of the anterior and posterior CB with the opacities was crucial for the analysis. Sectioning of this tissue had to be practiced with gentle handling. Furthermore, other immunohistochemical markers to identify whether mesenchymal cells under a mesenchymal to epithelial phenotypic reversion or under apoptosis should be performed to understand why there is lower expression of SMA with time. Other ECM proteins, such as laminin, vimentin, and collagen, should be assessed using the Positive Pixel Count algorithm to quantify their relative compositions in opacities present between different IOL types.

Biocompatibility is an important concept in determining the reaction of a non-biological substance in a biological structure. This compatibility between the IOL and the biological tissue of the CB is essential to understand to prevent opacification post-cataract surgery. Identifying those characteristics that influence this interaction can lead to a reduction in post-cataract surgery complications and further reduce the need for Nd:YAG laser capsulotomy, especially in countries with low accessibility to equipment and expert ophthalmology care. Taking the personalized medicine approach in the clinic can start today, and identifying higher potential factors that can influence CB interaction before cataract surgery can reduce the risk of post-cataract surgery complications such as PCO. Herein, by using objective immunohistochemical staining methods and software-based opacity grading, we determined associations and correlations between different IOL types, patient factors, and EMT factors that affect the composition of the CB of IOL transplanted eyes post-cataract surgery. Further comparisons between capsular opacities with both IOL and patient factors with a large series database are currently being completed by our laboratory this year.

Conclusion

In conclusion, by analyzing the histopathological composition of opacities and LEC changes, further insight into the characteristics of IOLs that are important for biocompatibility can be ascertained.

Acknowledgments

We are grateful to the Histopathology Core Facility at the McGill University Health Center Research Institute for the assistance with the embedding and sectioning of the slides. We thank Dr. Denise Miyamoto for her assistance in the design and the study concept, Dr. Mohamed Abdouh for his revisions, and Dr. Raman Agnihotram from the McGill University Health Center for helping with the statistical analysis.

Financial support and sponsorship

Nil.

Conflicts of interest

Mr. Balazsi reports that he has a patent null pending and is the founder of Medical Parachute, a company that offers software services to medical professionals. For this project, the MUHC-McGill University Ocular Pathology Laboratory employed the services of Medical Parachute along with their software to analyze the digital slides for a fee. Although the software has not been patented, Medical Parachute reserves the right to license the use of the software to other laboratories. All other authors report no conflicts of interest.

References

1. Lamoureux EL, Fenwick E, Pesudovs K, Tan D. The impact of cataract surgery on quality of life. *Curr Opin Ophthalmol* 2011;22:19-27.
2. Wang W, Yan W, Fotis K, Prasad NM, Lansingh VC, Taylor HR, *et al.* Cataract surgical rate and socioeconomics: A global study. *Invest Ophthalmol Vis Sci* 2016;57:5872-81.
3. Huang YS, Bertrand V, Bozukova D, Pagnoulle C, Labrugere C, De Pauw E, *et al.* RGD surface functionalization of the hydrophilic acrylic intraocular lens material to control posterior capsular opacification. *PLoS One* 2014;9:e114973.
4. Chandler HL, Barden CA, Lu P, Kusewitt DF, Colitz CM. Prevention of posterior capsular opacification through cyclooxygenase-2 inhibition. *Mol Vis* 2007;13:677-91.
5. Micallef L, Vedrenne N, Billet F, Coulomb B, Darby IA, Desmouliere A. The myofibroblast, multiple origins for major roles in normal and pathological tissue repair. *Fibrogenesis Tissue Repair* 2012;5(Suppl 1):S5.
6. Saika S, Werner L, Lovicu FJ. Lens Epithelium and Posterior Capsular Opacification. SpringerLink (Online service). Available from: <http://dx.doi.org/10.1007/978-4-431-54300-8>.
7. Saika S, Okada Y, Miyamoto T, Ohnishi Y, Ooshima A, McAvoy JW. Smad translocation and growth suppression in lens epithelial cells by endogenous TGFbeta2 during wound repair. *Exp Eye Res* 2001;72:679-86.
8. Xiao W, Chen X, Li W, Ye S, Wang W, Luo L, *et al.* Quantitative analysis of injury-induced anterior subcapsular cataract in the mouse: A model of lens epithelial cells proliferation and epithelial-mesenchymal transition. *Sci Rep* 2015;5:8362.
9. Saika S. Relationship between posterior capsule opacification and intraocular lens biocompatibility. *Prog Retin Eye Res* 2004;23:283-305.
10. Bhattacharjee H, Bhattacharjee K, Das D, Singh M, Sukumar P, Misra DK. Pathology and immunohistochemistry of capsular bag in spontaneously late dislocated capsular bag-intraocular lens complex. *Indian J Ophthalmol* 2017;65:949-54.
11. Matsushima H, Mukai K, Obara Y, Yoshida S, Clark JI. Analysis of cytoskeletal proteins in posterior capsule opacification after implantation of acrylic and hydrogel intraocular lenses. *J Cataract Refract Surg* 2004;30:187-94.
12. Linnola RJ, Sund M, Ylonen R, Pihlajaniemi T. Adhesion of soluble fibronectin, vitronectin, and collagen type IV to intraocular lens materials. *J Cataract Refract Surg* 2003;29:146-52.
13. Saika S, Miyamoto T, Ohnishi Y. Histology of anterior capsule opacification with a polyHEMA/HOHEXMA hydrophilic hydrogel intraocular lens compared to poly (methyl methacrylate), silicone, and acrylic lenses. *J Cataract Refract Surg* 2003;29:1198-203.
14. Linnola RJ, Werner L, Pandey SK, Escobar-Gomez M, Znoiko SL, Apple DJ. Adhesion of fibronectin, vitronectin, laminin, and collagen type IV to intraocular lens materials in pseudophakic human autopsy eyes. Part 1: Histological sections. *J Cataract Refract Surg* 2000;26:1792-806.
15. Mastromonaco C, Balazsi M, Zoroquiain P, Esposito E, Coblenz J, Logan P, *et al.* Removing subjective post-mortem grading from posterior capsular opacification: A new automated detector opacification software, ADOS. *Curr Eye Res* 2018;43:1362-8.
16. Werner L, Pandey SK, Escobar-Gomez M, Visessook N, Peng Q, Apple DJ. Anterior capsule opacification: A histopathological study comparing different IOL styles. *Ophthalmology* 2000;107:463-71.
17. Zoroquiain P, Logan P, Bravo-Filho V, Vila N, Jabbour S, Orellana ME, *et al.* Diagnosing pathological prognostic factors in retinoblastoma: Correlation between traditional microscopy and digital slides. *Ocul Oncol Pathol* 2015;1:259-65.

18. Farris AB, Cohen C, Rogers TE, Smith GH. Whole slide imaging for analytical anatomic pathology and telepathology: Practical applications today, promises, and perils. *Arch Pathol Lab Med* 2017;141:542-50.
19. Brazdziute E, Laurinavicius A. Digital pathology evaluation of complement C4d component deposition in the kidney allograft biopsies is a useful tool to improve reproducibility of the scoring. *Diagn Pathol* 2011;6(Suppl 1):S5.
20. Dunn WD Jr, Gearing M, Park Y, Zhang L, Hanfelt J, Glass JD, *et al.* Applicability of digital analysis and imaging technology in neuropathology assessment. *Neuropathology* 2016;36:270-82.
21. Garcia-Rojo M, Sanchez J, de la Santa E, Duran E, Ruiz JL, Silva A, *et al.* Automated image analysis in the study of lymphocyte subpopulation in eosinophilic oesophagitis. *Diagn Pathol* 2014;9(Suppl 1):S7.
22. Werner L, Pandey SK, Apple DJ, Escobar-Gomez M, McLendon L, Macky TA. Anterior capsule opacification: Correlation of pathologic findings with clinical sequelae. *Ophthalmology* 2001;108:1675-81.
23. Ishibashi T, Araki H, Sugai S, Tawara A, Ohnishi Y, Inomata H. Anterior capsule opacification in monkey eyes with posterior chamber intraocular lenses. *Arch Ophthalmol* 1993;111:1685-90.
24. Marcantonio JM, Rakic JM, Vrensen GF, Duncan G. Lens cell populations studied in human donor capsular bags with implanted intraocular lenses. *Invest Ophthalmol Vis Sci* 2000;41:1130-41.
25. Law SM, Lu X, Yu F, Tseng V, Law SK, Coleman AL. Cigarette smoking and glaucoma in the United States population. *Eye (Lond)* 2018;32:716-25.
26. Chen HC, Lee CY, Sun CC, Huang JY, Lin HY, Yang SF. Risk factors for the occurrence of visual-threatening posterior capsule opacification. *J Transl Med* 2019;17:209.
27. Hoehn R, Mirshahi A, Hoffmann EM, Kottler UB, Wild PS, Laubert-Reh D, *et al.* Distribution of intraocular pressure and its association with ocular features and cardiovascular risk factors: The Gutenberg health study. *Ophthalmology* 2013;120:961-8.
28. Hillenmayer A, Wertheimer CM, Kassumeh S, von Studnitz A, Luft N, Ohlmann A, *et al.* Evaluation of posterior capsule opacification of the Alcon Clareon IOL vs the Alcon Acrysof IOL using a human capsular bag model. *BMC Ophthalmol* 2020;20:77.
29. Cooke CA, McGimpsey S, Mahon G, Best RM. An *in vitro* study of human lens epithelial cell adhesion to intraocular lenses with and without a fibronectin coating. *Invest Ophthalmol Vis Sci* 2006;47:2985-9.
30. Gotoh N, Perdue NR, Matsushima H, Sage EH, Yan Q, Clark JJ. An *in vitro* model of posterior capsular opacity: SPARC and TGF-beta2 minimize epithelial-to-mesenchymal transition in lens epithelium. *Invest Ophthalmol Vis Sci* 2007;48:4679-87.
31. Lee EH, Joo CK. Role of transforming growth factor-beta in transdifferentiation and fibrosis of lens epithelial cells. *Invest Ophthalmol Vis Sci* 1999;40:2025-32.
32. Shu DY, Lovicu FJ. Myofibroblast transdifferentiation: The dark force in ocular wound healing and fibrosis. *Prog Retin Eye Res* 2017;60:44-65.
33. Ma B, Jing R, Liu J, Yang L, Li J, Qin L, *et al.* CTGF contributes to the development of posterior capsule opacification: An *in vitro* and *in vivo* study. *Int J Biol Sci* 2018;14:437-48.
34. Mamuya FA, Wang Y, Roop VH, Scheiblin DA, Zajac JC, Duncan MK. The roles of alphaV integrins in lens EMT and posterior capsular opacification. *J Cell Mol Med* 2014;18:656-70.
35. Chen KC, Zhou Y, Zhang W, Lou MF. Control of PDGF-induced reactive oxygen species (ROS) generation and signal transduction in human lens epithelial cells. *Mol Vis* 2007;13:374-87.
36. Zukin LM, Pedler MG, Groman-Lupa S, Pantcheva M, Ammar DA, Petrash JM. Aldose reductase inhibition prevents development of posterior capsular opacification in an *in vivo* model of cataract surgery. *Invest Ophthalmol Vis Sci* 2018;59:3591-8.